



RESEARCH LETTER

10.1029/2019GL083802

Pliocene Warmth Consistent With Greenhouse Gas Forcing

Key Points:

- Pliocene SSTs calculated from the alkenone proxy do not support a “permanent El Niño”
- Pliocene model simulations can reproduce proxy-inferred SST patterns and gradients
- The pattern of Pliocene warmth supports a weakening of Walker circulation under higher CO₂

Supporting Information:

- Supporting Information S1
- Data Set S1
- Data Set S2
- Data Set S3

Correspondence to:

J. E. Tierney,
jesst@email.arizona.edu

Citation:

Tierney, J. E., Haywood, A. M., Feng, R., Bhattacharya, T., & Otto-Bliesner, B. L. (2019). Pliocene warmth consistent with greenhouse gas forcing. *Geophysical Research Letters*, 46, 9136–9144. <https://doi.org/10.1029/2019GL083802>

Received 20 MAY 2019

Accepted 25 JUL 2019

Accepted article online 1 AUG 2019

Published online 14 AUG 2019

Jessica E. Tierney¹, Alan M. Haywood², Ran Feng³, Tripti Bhattacharya⁴, and Bette L. Otto-Bliesner⁵

¹Department of Geosciences, University of Arizona, Tucson, AZ, USA, ²School of Earth and Environment, University of Leeds, Leeds, UK, ³Department of Geosciences, University of Connecticut, Storrs, CT, USA, ⁴Department of Earth Sciences, Syracuse University, Syracuse, NY, USA, ⁵National Center for Atmospheric Research, Boulder, CO, USA

Abstract With CO₂ concentrations similar to today (410 ppm), the Pliocene Epoch offers insights into climate changes under a moderately warmer world. Previous work suggested a low zonal sea surface temperature (SST) gradient in the tropical Pacific during the Pliocene, the so-called “permanent El Niño.” Here, we recalculate SSTs using the alkenone proxy and find moderate reductions in both the zonal and meridional SST gradients during the mid-Piacenzian warm period. These reductions are captured by coupled climate model simulations of the Pliocene, especially those that simulate weaker Walker circulation. We also produce a spatial reconstruction of mid-Piacenzian warm period Pacific SSTs that closely resembles both Pliocene and future, low-emissions simulations, a pattern that is, to a first order, diagnostic of weaker Walker circulation. Therefore, Pliocene warmth does not require drastic changes in the climate system—rather, it supports the expectation that the Walker circulation will weaken in the future under higher CO₂.

Plain Language Summary The Pliocene Epoch is the most recent time in Earth history when CO₂ levels exceeded 400 ppm. The climate was warmer than preindustrial times, with smaller ice sheets. Previous studies suggested that the Pacific ocean was stuck in a “permanent El Niño” during the Pliocene. However, climate model simulations do not predict that this would happen at CO₂ levels near 400 ppm—unusual changes in climate, such as large changes in cloud cover or hurricane frequency, would be needed to explain it. In this work we reanalyze Pliocene sea surface temperature data and do not find evidence of a permanent El Niño. Our results suggest that difference in temperatures across the tropical Pacific was smaller than it is today, but only by about 1 °C. Climate model simulations agree with our new analysis, suggesting that higher CO₂, along with small changes in ice, vegetation, and mountains, is enough to explain Pliocene climate. We also show that the sea surface temperature patterns in the Pliocene Pacific Ocean look similar to those that climate models predict under a low-emissions climate change scenario. The similarity suggests that the Pliocene can help us understand how the tropics respond to an ongoing increase in CO₂.

1. Introduction

As an equilibrated climate state under CO₂ levels (300–450 ppm; Foster et al., 2017) similar to the current value (410 ppm), the Pliocene Epoch (5.3–2.6 Ma) offers useful insights into the climate dynamics of the near future. One intriguing feature of the Pliocene is evidence of a “permanent El Niño” in the tropical Pacific (Fedorov et al., 2006; Wara et al., 2005), that is, a severe reduction to near elimination of the average east-west temperature gradient along the equator. However, the magnitude of this reduction is uncertain, with some studies suggesting only a moderate change (O’Brien et al., 2014; Zhang et al., 2014), while others confirm the original estimate (Brierley et al., 2015; Ravelo et al., 2014). Resolving this debate is important, because CO₂ forcing alone cannot explain the Pliocene permanent El Niño. Changes not simulated by current state-of-the-art models, such as enhanced tropical cyclone activity (Fedorov et al., 2010), and extreme changes in cloud albedo (Burls & Fedorov, 2014) are needed to produce a strong reduction in the Pacific sea surface temperature (SST) gradient. If such shifts took place in the Pliocene, they could become active in the warmer future, with implications for climate prediction.

©2019. The Authors.

This is an open access article under the terms of the Creative Commons Attribution License, which permits use, distribution and reproduction in any medium, provided the original work is properly cited.

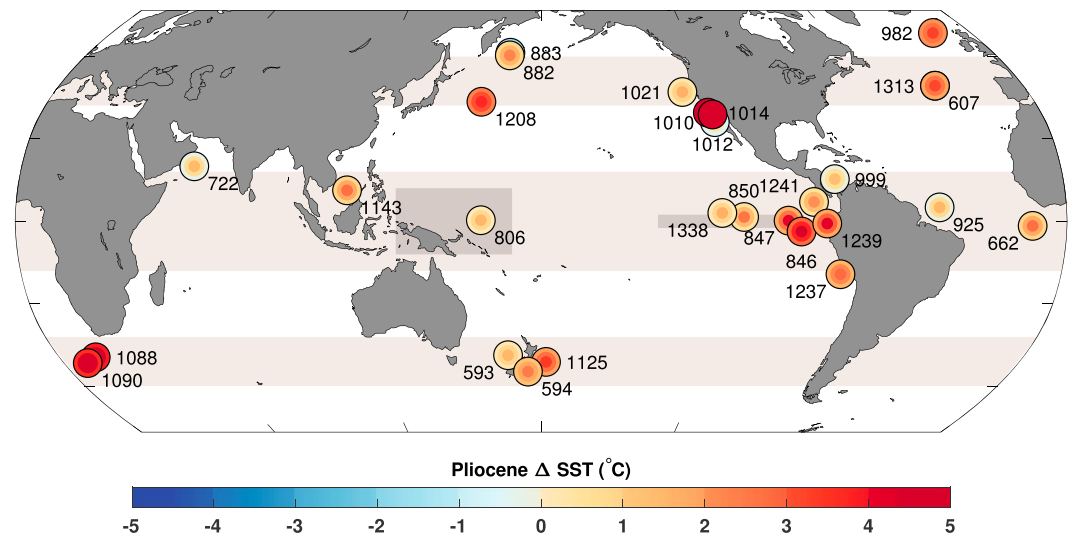


Figure 1. Pliocene SST anomalies (mid-Piacenzian–preindustrial, calculated from $U_{37}^{K'}$) at the core sites used in this study. Sites are labeled with their Deep Sea Drilling Project, Ocean Drilling Project, or Integrated Ocean Drilling Project number. Layered circles show the 2.5% (outside ring), 50% (median, middle ring), and 95% confidence levels (inner circle) for each site. Shaded bands and darker boxes mark the tropical and midlatitude regions, and western and eastern Pacific regions, used for model box averages, respectively. SST = sea surface temperature.

Here, we recalculate Pliocene patterns of warmth and SST gradients using a single proxy and a probabilistic approach. Given controversies associated with the Mg/Ca and TEX_{86} paleothermometers (O'Brien et al., 2014; Ravelo et al., 2014) we base our reconstruction solely on alkenone ($U_{37}^{K'}$) paleothermometric data, an established proxy for SSTs. Eighty-three percent of the SST records from the Pliocene have $U_{37}^{K'}$ measurements, providing global coverage (Figure 1). The main limitation of $U_{37}^{K'}$ is that it has an upper bound of $\sim 30^\circ\text{C}$, challenging inference in warm waters. However, a new Bayesian calibration, BAYSPLINE, improves prediction of SSTs near the saturation point (Tierney & Tingley, 2018) and allows us to generate probabilistic representations of Pliocene SSTs that fully incorporate uncertainties in the $U_{37}^{K'}$ proxy.

Following Fedorov et al. (2015), we reconstruct SST anomalies from key regions (eastern Pacific, western Pacific, tropics, and midlatitudes) as well as zonal and meridional gradients. We investigate the meridional SST gradient (tropics—midlatitudes) because one mechanism for the permanent El Niño involves strong subtropical warming, which would feed warm waters into the tropical Pacific thermocline and reduce the zonal gradient (Burls & Fedorov, 2014; Fedorov et al., 2015). We focus on the mid-Piacenzian warm period (MPWP, 3.264–3.025 Ma; Dowsett et al., 2010), because the Pliocene Model Intercomparison Project 1 (PlioMIP1; Haywood et al., 2013) targeted this specific time. We use model output from PlioMIP1 and a new simulation conducted with the Community Earth System Model (CESM1-CAM5) to compare with proxy-derived estimates. We aim to assess (1) whether there was a permanent El Niño, and (2) more generally, whether simulations forced with standard MPWP boundary conditions can reproduce proxy SST anomalies.

2. Materials and Methods

2.1. Alkenone Proxy Approach

Our SST anomaly reconstructions are based on published alkenone $U_{37}^{K'}$ data from 28 sites (Figure 1 and supporting information Table S1). We use these data to reconstruct regional SST anomalies and the Pacific SST field (see section 2.3). The regions targeted include the midlatitudes, following the definition in Fedorov et al. (2015; $30^\circ\text{--}50^\circ\text{N}$ or $^\circ\text{S}$, excludes subtropical upwelling zones, includes Site 982 at 57°N), the eastern equatorial Pacific, the western Pacific warm pool, and the tropics (see Table S1 for a list of sites assigned to each region). Our analysis is limited to the last 4 Ma because prior to this time, only one site is available in the western Pacific (ODP 806) and this biases the regional average. We calibrated $U_{37}^{K'}$ data to SSTs using BAYSPLINE (Tierney & Tingley, 2018) with a prior standard deviation of 5°C , a loose prior that only minimally impacts the posterior. For each site, anomalies were calculated relative to a preindustrial estimate of SST, which, wherever possible, was based on a coretop or latest Holocene $U_{37}^{K'}$ value (see Text S1). In order to

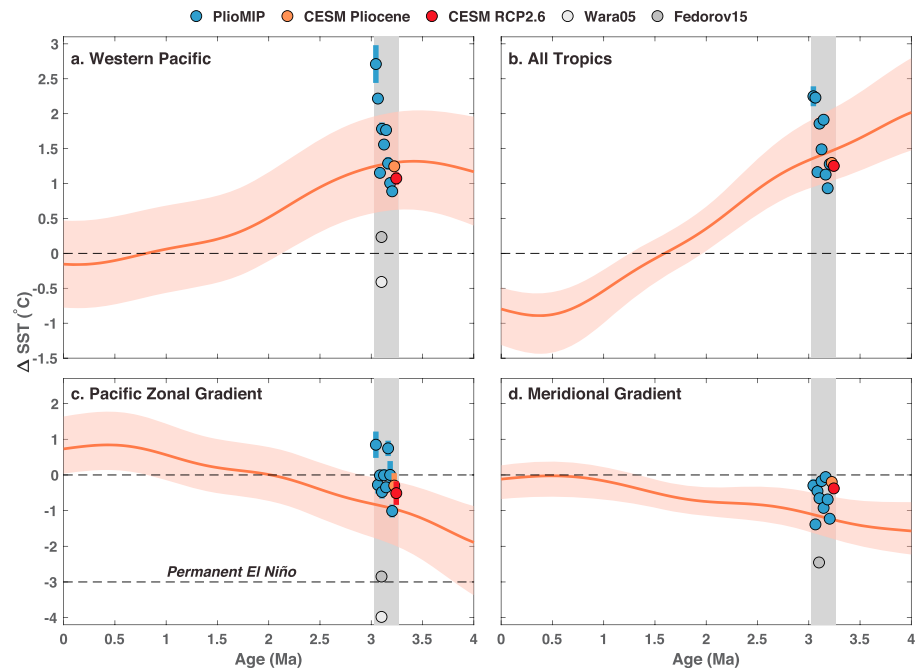


Figure 2. Reconstruction of SST anomalies and gradients for the past 4 Ma from $U_{37}^{K'}$ data and comparison to model simulations. Each panel shows anomalies relative to preindustrial. A Gaussian smoothing of 400 ka was applied to the reconstructions; note that smoothed data do not equal 0 at 0 Ma because they average glacial-interglacial cycles. Shaded areas represent the 95% confidence interval. Gray bar encloses the mid-Pliocene warm period. Blue dots show PlioMIP1 model simulations; orange and red dots show CESM Pliocene and RCP2.6 simulations, respectively. Model estimates are offset from one another for clarity and are plotted with 2σ error bars that account for interannual variability. Gray dots show previous estimates from Wara et al. (2005) and Fedorov et al. (2015). The “Permanent El Niño” threshold of -3°C in anomaly space is equivalent to an absolute west-east gradient of 1.2°C (see main text). SST = sea surface temperature; CESM = Community Earth System Model; RCP = Representative Concentration Pathway.

equally weight the contribution of each site, data were interpolated to a common time step of 5 ka between 0 and 4 Ma prior to taking a regional average. To emphasize long-term (supra-orbital) variability, a 400-ka (full-width, 6σ) Gaussian smoothing is applied to these estimates in Figure 2. To assess whether the proxy data indicate a permanent El Niño, we formally define this as a zonal gradient of less than 1.2°C , the average gradient during the strongest historically observed El Niño events (1877, 1982, 1997, and 2015). This limit is calculated from the ERSSTv5 product (Huang et al., 2017), using the same regional averages as the model simulations (see section 2.2).

2.2. Climate Model Simulations

We analyzed simulated SSTs from nine models participating in PlioMIP1 Experiment 2, run under 405 ppm CO_2 (Haywood et al., 2011). The other boundary conditions for the experiment are based on the PRISM3D reconstruction (Dowsett et al., 2010) and described in Haywood et al. (2010, 2011); see also Text S2. We also use results from a new Pliocene simulation run with CESM1 (Hurrell et al., 2013), under the same boundary conditions as PlioMIP1 Experiment 2 (see Text S2), and the extended Representative Concentration Pathway (RCP) 2.6 simulation conducted with CESM1 as part of the CMIP5 effort (Meinshausen et al., 2011; Taylor et al., 2012). RCP2.6 is an aggressive mitigation scenario, under which CO_2 concentrations peak at ~ 450 ppm by 2050 and then decline to 360 ppm by 2300. These CO_2 levels are similar to Pliocene values (300–450 ppm; Foster et al., 2017). For all experiments, we analyze the last 50 years of the simulation. To compare model output with the regional alkenone reconstructions, we take box averages across the regions of interest, including the western Pacific warm pool (10°S – 10°N , 130 – 170°E), the tropics (15°S – 15°N), the eastern equatorial Pacific cold tongue (2°S – 2°N , 140 – 90°W) and the midlatitudes (50 – 35°S , 35 – 50°N) (Figure 1). Median anomalies and 2σ standard errors (based on bootstrap estimates of annual data) are used to compare the model output with the proxy data. Box averages are preferred over using output from the individual site locations because they are less sensitive to model-specific biases in the Pacific cold tongue, warm pool, and midlatitude fronts; however, our results are not sensitive to this choice (see Text S2).

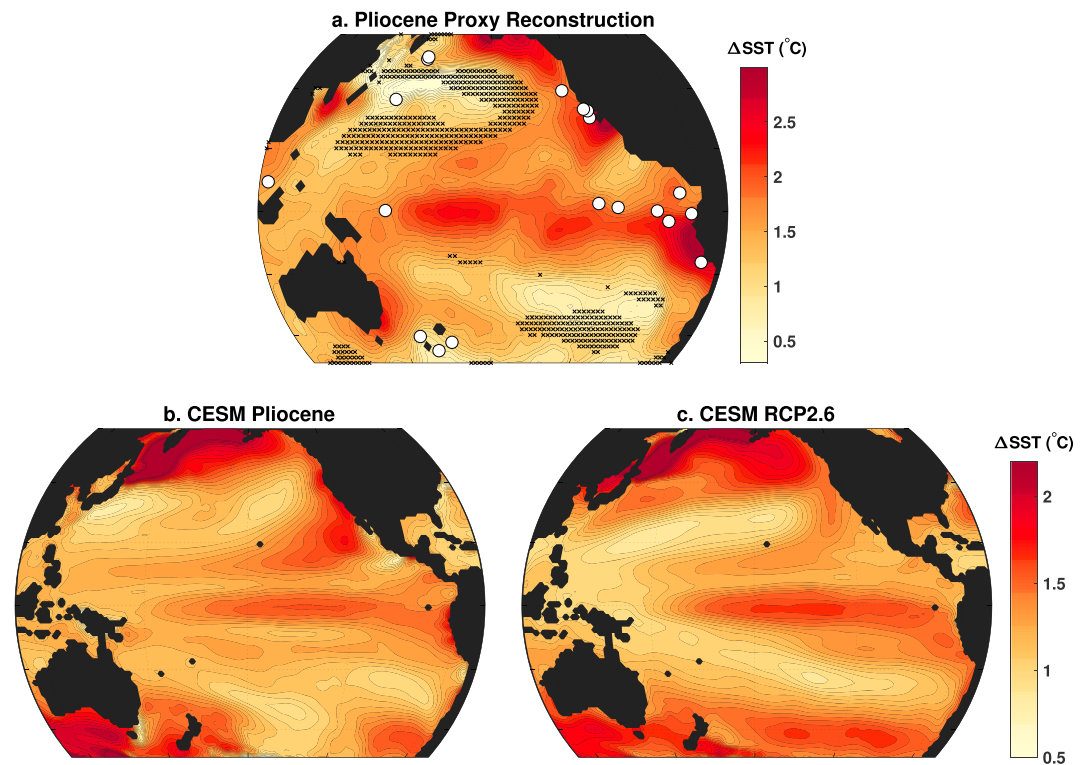


Figure 3. Reconstructed and simulated Pacific SST anomalies relative to preindustrial conditions. (a) Reduced space reconstruction (median field) of mid-Piacenzian warm period SST anomalies using alkenone proxy data (white dots). Hashed areas denote regions without skill ($RE < 0$; Figure S3b). (b) SST anomalies from the CESM Pliocene simulation. (c) SST anomalies (average from 2250–2300 CE) from the CESM RCP2.6 simulation. SST = sea surface temperature; CESM = Community Earth System Model; RCP = Representative Concentration Pathway.

2.3. Reduced Space Reconstruction

To create a field reconstruction of Pliocene SST anomalies, we follow the reduced space methodology of Gill et al. (2016) with modifications to propagate proxy uncertainties and accommodate Bayesian inference. The reduced space method uses the leading EOFs of historical SST variability—including the global warming signature and patterns associated with El Niño (Figure S1)—in order to reconstruct the Pliocene Pacific SST field. We posit that this is a reasonable assumption, as Pliocene continental configuration is similar to present day, and the leading EOFs in the CESM1 preindustrial and Pliocene SST simulations are similar (Figure S2). Briefly, the method proceeds as follows: Pacific SST anomalies from the ERSSTv5 product (Huang et al., 2017) are subject to singular value decomposition, alongside a limited field that consists only of the locations where there are Pliocene proxy data. The leading principal components (PCs) of the limited field are used to predict the PCs of the full field using Bayesian linear regression. The Pliocene proxy SST anomalies are then converted to PC space, and the regressions are used to predict full field PCs. The full field for the Pliocene is computed from eigenvalue expansion. Mathematical details are provided in Text S3.

3. Results

Our reconstructed regional SST anomalies indicate that the western Pacific warm pool was $1.3\text{ }^{\circ}\text{C}$ (95% confidence interval (CI) = 0.6 to $2.0\text{ }^{\circ}\text{C}$, Figure 2a) warmer than preindustrial during the MPWP, similar to the tropics as a whole ($1.4\text{ }^{\circ}\text{C}$, 95% CI = 1.0 to $2.0\text{ }^{\circ}\text{C}$, Figure 2b). The magnitude of warming in the eastern Pacific and midlatitudes is larger, such that there is a moderate but significant decrease in both the tropical Pacific zonal gradient ($-0.9\text{ }^{\circ}\text{C}$, 95% CI = -1.9 to $-0.1\text{ }^{\circ}\text{C}$) and the meridional gradient ($-1.2\text{ }^{\circ}\text{C}$, 95% CI = -1.7 to $-0.6\text{ }^{\circ}\text{C}$; Figures 2c and 2d). Our estimate for the change in the zonal gradient is well above the threshold for a permanent El Niño (Figure 2c). The proxy-inferred anomalies compare favorably with simulations of MPWP climate from PlioMIP and CESM1 (Figure 2). The majority of the models predict warm pool, tropical, and zonal gradient anomalies within the 95% CI of the proxy estimates (8/10). Half of the models produce a meridional gradient reduction within the 95% range (5/10). CESM predictions for

years 2250–2300 under RCP 2.6 show a warming in the western Pacific and tropics and a decrease in the zonal gradient that are similar to the Pliocene data and simulations (1.1 °C, 1.3 °C, and –0.5 °C, respectively; Figure 2).

The reduced space reconstruction shows enhanced warming in the eastern equatorial Pacific cold tongue and the Peru and California margin upwelling zones and a horseshoe pattern of warming that extends up the Alaskan margin and southwestward across the northern subtropical Pacific (Figure 3a). Compared to the PRISM3 reconstruction, our SST anomalies are 1–2 °C warmer in the tropics and 1–3 °C cooler in the subtropics (Figure S3). For model comparison, we focus on CESM1, which simulates a zonal gradient reduction within range of the proxy estimates (Figure 2c). The same spatial features—enhanced warming in the northeast Pacific and eastern equatorial region—are clearly seen in the simulations of both the MPWP and RCP 2.6 (Figures 3b and 3c). The magnitudes of the simulated anomalies are smaller than the median field, but well within uncertainty of the reconstruction (Figure S4a). The model simulations show different responses in the northwest Pacific and southern Ocean (Figure 3); however, our reconstruction has limited skill (and data) in these regions (Figure S4b). Across the tropics and the subtropics (35°S to 35°N), where most proxy data lie and the reconstruction has the strongest skill, the correlation between the reconstructed anomalies and the CESM Pliocene anomalies is 0.71.

4. Discussion

Overall, our new reconstructions of Pliocene SSTs show good agreement with model simulations during the MPWP. Most models can reproduce the magnitude of warm pool and tropical warmth and moderate zonal gradient reduction (Figure 2). Some models do underestimate the decrease in the zonal or meridional gradient, but the mismatch is not as large as previously thought (Figures 2c and 2d). Notably, the RCP2.6 simulation with CESM1 results in Pliocene-like warming and zonal gradient reduction (Figure 2). Although Pliocene changes in orography, ice, and vegetation contribute to a rise in global mean air temperature (Lunt et al., 2012), the impact of these effects on SSTs is smaller, especially in the tropics and subtropics. Our results with CESM1 suggest that for the regions of interest here, Pliocene CO₂ forcing is dominant.

Our results support the inferences based on the TEX₈₆ paleothermometer that the Pliocene Pacific zonal gradient was moderately lower than preindustrial (~ –1 °C; O'Brien et al., 2014; Zhang et al., 2014) and disagree with studies that have argued for a –3 to –4 °C change (Fedorov et al., 2015; Wara et al., 2005) consistent with a permanent El Niño (Figure 2c). The difference between our result and the latter work can be attributed to several factors. The first is our use of BAYSPLINE, which ameliorates the tendency of previous U₃₇^{K'} calibrations (e.g., Müller et al., 1998) to underestimate tropical SSTs (Tierney & Tingley, 2018), produces warmer estimates for tropical U₃₇^{K'} sites during the Pliocene (Figure S5), and therefore yields smaller zonal and meridional gradient anomalies. We acknowledge that, at Sites 1143 and 806, U₃₇^{K'} is close to, and occasionally reaches, its limit (a value of 1). In the BAYSPLINE calibration, the limit does not correspond to a single value of SST but rather is probabilistically estimated to be 30.4 °C ± 5.5 °C (2σ). However, comparison between U₃₇^{K'}-inferred SSTs and two other paleothermometers (TEX₈₆ and Mg/Ca with a seawater adjustment) at these sites shows good agreement in the MPWP (Figure S5). This confirms that our choice to focus on a single proxy (U₃₇^{K'}) does not skew our results.

In the western Pacific warm pool, previous work relied on analysis of faunal assemblages (Dowsett et al., 2009, 2011) or the Mg/Ca paleothermometer (Fedorov et al., 2015; Wara et al., 2005) and found either no evidence for warmer temperatures than preindustrial or a cooling relative to preindustrial (e.g., Figures 2a and S2). However, faunal assemblage methods cannot by design predict temperatures above their calibration range (Dowsett, 2007), and Mg/Ca inferences did not account for the increase in Mg/Ca of seawater (Mg/Ca_{sw}) over the last several million years (Evans et al., 2016). Both factors cause systematic underestimation of western Pacific warming during the Pliocene and a greater inferred reduction in the zonal gradient. Since Mg/Ca sensitivity to temperature is nonlinear, the change in Mg/Ca_{sw} has a bigger impact on the warmer western Pacific sites than the eastern Pacific sites. This results in artificially small gradient calculations, even if only Mg/Ca data are used. The sensitivity of Mg/Ca to other environmental factors, including salinity, pH, and dissolution (Gray et al., 2018; Regenberg et al., 2014), may further confound SST inference (O'Brien et al., 2014).

Another factor contributing to the more moderate results in our study is that we consider anomalies relative to preindustrial conditions for the MPWP specifically so that we can make a proportionate comparison to

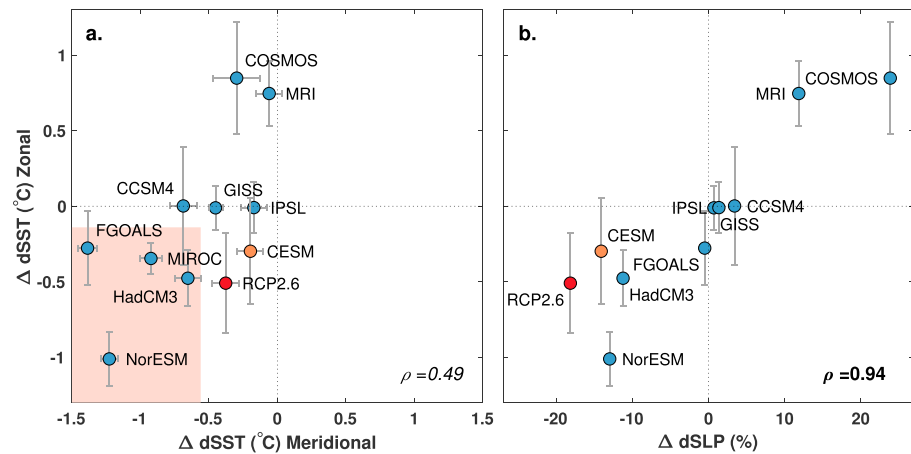


Figure 4. The Pacific zonal SST gradient change versus the meridional SST gradient change (a) and sea level pressure gradient (a proxy for Walker circulation) change across the equatorial Pacific (5°S to 5°N, 80–140°W–5°S to 5°N, 155–180°E; b) across model simulations. Error bars represent the 2σ bootstrap uncertainties. Pink box in panel (a) encloses the proxy-inferred range of values for the mid-Piacenzian warm period. The MIROC model is not plotted in (b) because sea level pressure data were not available. Spearman ρ correlations are shown in the lower right corner; the value in panel (a) is not significant ($p = 0.13$). SST = sea surface temperature.

the model simulations. Previous work estimated gradient changes using a running mean that smoothed over Late Pleistocene glacial cycles (Brierley et al., 2015; Fedorov et al., 2015). This includes the impact of glaciation and therefore yields larger anomalies. Previous work also compared proxy data spanning all of the Pliocene, 5.3–2.6 Ma, to the model simulations, even though CO_2 levels may have changed over this period. This said, if we extend our proxy average to 4–2.6 Ma, we obtain similar results: the zonal gradient changes by -1.1°C (95% CI = -2.2 to -0.28°C) and the meridional gradient by -1.3°C (95% CI = -1.8 to -0.60°C).

A final difference is our choice to include all available sites in the western and eastern Pacific regional averages. In our view, this is the most methodologically defensible approach, as it ensures that random noise associated with a single proxy site, and/or genuine but localized variations in SST, have less impact on the averages. In particular, there has been debate over whether Site 1143, located in the South China Sea (Figure 1), is representative of the western Pacific (Brierley et al., 2015; O'Brien et al., 2014; Zhang et al., 2014). Based on analysis of the ERSSTv5 product, Site 1143 has a mean annual preindustrial SST of 28.1°C , and SST variability is strongly correlated with the open-water warm pool (10°S – 10°N , 130 – 170°E ; $r = 0.66$, $p \ll 0.0001$), and Site 806 ($r = 0.60$, $p \ll 0.0001$). This site also sits underneath the ascending branch of the Walker cell. For these reasons, we retain Site 1143 in our regional average; however, our results are not sensitive to this choice (Figure S6).

Previous work suggested that the reduction in the Pacific zonal gradient during the Pliocene is closely tied to changes in the meridional gradient; that is, entrainment of warm subtropical waters into the Pacific thermocline drives a relaxation of the zonal gradient (Burls & Fedorov, 2014; Fedorov et al., 2015). However, we do not find a significant relationship between the meridional and zonal SST gradients across models (Figure 4a). Likewise, while the proxy data indicate that both the zonal and meridional gradients decrease back in time, the changes in the zonal gradient are larger (by about a factor of 2; Figures 2c and 2d). In the model simulations, the change in the sea level pressure gradient across the Pacific—a proxy for the Walker Circulation—is a stronger predictor of zonal gradient change than the meridional gradient (Figure 4b). This underscores the importance of tropical rather than extratropical ocean-atmosphere dynamics in driving a reduced zonal gradient during the Pliocene.

There is a notable diversity in the zonal gradient response across the models (Figure 4b), with two models predicting an increase during the Pliocene. This could reflect cold tongue bias, which impacts both the direction and magnitude of zonal gradient change in response to elevated CO_2 (Li et al., 2016). Models with an exaggerated cold tongue tend to simulate smaller reductions in the gradient or even a strengthened gradient, because they underestimate precipitation in the western Pacific and therefore overestimate warming in that area (Li et al., 2016). This may explain the behavior of the COSMOS model, which has a cold tongue that extends to Indonesia. It predicts overly strong warming in the western Pacific with

a high standard deviation (2.7 ± 0.27 °C; Figure 2a) and a strengthened gradient. However, across the remaining PlioMIP models there is no relationship between western Pacific warming and the zonal gradient change ($\rho = -0.08$). There is also no significant relationship between bias in cold tongue temperature (assessed relative to ERSSTv5, 1854–1900), nor bias in the longitudinal extent of the cold tongue (assessed as the location of the 28 °C isotherm at the equator), and the simulated zonal gradient change, respectively ($\rho = 0.01$, $\rho = -0.21$, $p > 0.5$ in both cases). This suggests to us that cold tongue bias is not responsible for the model diversity.

Rather, to a first order the magnitude of zonal gradient change in each model is directly related to its Walker circulation change (Figure 4b). We suspect that the diversity of Walker response across models reflects different parameterizations that impact convection, cloud feedbacks, evaporative damping, and ocean-atmosphere coupling in the tropics. Comparison between CCSM4 and CESM1 is illustrative in this respect, as these models differ only in the generation of atmospheric model used. CESM1, which incorporates updated cloud parameterizations and microphysics (Gettelman, 2015), simulates a much stronger weakening of the Walker circulation (Figure S7).

CESM1 also produces a pattern of MPWP warmth in the Pacific that closely resembles our field reconstruction (Figures 3a and 3b). The RCP2.6 simulation is similar (Figure 3c), which suggests that the common forcing—higher CO₂ concentrations—is primarily responsible for these changes. In both simulations, the preferential warming of the cold tongue and reduction in the zonal SST gradient arises from a weakening of the Walker circulation (Figure S8), a well-known response to elevated greenhouse gases (DiNezio et al., 2009; Knutson & Manabe, 1995; Vecchi & Soden, 2007). The strong warming off of California, extending across the northeast Pacific—a prominent feature in our spatial reconstruction and the model output—is accompanied by rising air in the CESM1 simulations (Figures S8c and S8d) and is linked to weaker Walker circulation via an “atmospheric bridge”—the propagation of pressure changes from the tropics to the extratropics by large-scale Rossby waves (Lau & Nath, 1996). Southerly wind anomalies associated with lower pressure off of California and Peru cause warming by altering air-sea heat exchange and reducing Ekman pumping (Lau & Nath, 1996; Figure 3). The advection of warm waters from higher latitudes and warming of the thermocline further amplifies this response (Figure S9). Along the California margin, cloud feedbacks, which are particularly active in the atmospheric model (CAM5) used by CESM1 (Gettelman et al., 2012), result in reduced low clouds, increasing shortwave radiation flux, and enhanced warming (Figure S10). This low-level cloud feedback is consistent with twentieth-century observations in the northeast Pacific (Clement et al., 2009) as well as emerging consensus that cloud feedbacks play an important role in warm climates (Bretherton, 2015; Schneider et al., 2019).

5. Conclusions

In summary, we find that climate model simulations can reproduce tropical warming, zonal gradient reduction, and the spatial fingerprint of Pacific SST anomalies during the MPWP. This suggests that standard Pliocene boundary conditions are adequate explanations for proxy observations. This does not exclude a role for clouds and tropical cyclones; indeed, in our simulations, cloud feedbacks are key for promoting warming in the northeast Pacific, in agreement with previous work (Burls & Fedorov, 2014, 2017), and cyclone intensity is expected to increase under high CO₂ (Emanuel et al., 2008). However, our proxy model analysis suggests that drastic changes in clouds or ocean mixing are not needed to explain Pliocene warmth.

While weaker Walker circulation is observed in most future climate simulations (Vecchi & Soden, 2007), by some accounts twentieth-century observations show a strengthening of circulation, raising questions as to whether the simulated projections represent reality (Karnauskas et al., 2009; Seager et al., 2019). Here we show that the pattern of SST change during the Pliocene clearly supports a weakening of Walker circulation under elevated CO₂. This finding agrees with recent reanalyses that suggest the strengthening of the Walker circulation observed in the last few decades (L'Heureux et al., 2013) is due to internal variability, not CO₂ forcing (Chung et al., 2019). Not all simulations of the Pliocene show weaker Walker (Figure 4b), highlighting the importance of model parameterizations (Figure S7).

The weakening of Walker circulation does not impact El Niño variance in the Pliocene CESM simulations; in fact, median NINO3.4 SST variance is slightly higher in the Pliocene compared to the preindustrial simulation (0.79 vs. 0.56). This differs from the PlioMIP simulations, which show either no change or a slight reduction in NINO3.4 variance (Brierley, 2015). However, none of the models indicate that El Niño disappears,

in agreement with proxy coral evidence (Watanabe et al., 2011). Neither the mean state nor the variance of Pliocene SSTs supports a permanent El Niño.

RCP2.6—a “Pliocene-like” climate state—is an optimistic scenario. It assumes that society adopts aggressive mitigation involving net negative emissions to maintain and/or reduce CO₂ to levels around 360–400 ppm. For higher levels of emissions, Walker circulation and temperature gradients might weaken further, but this remains to be tested. Broadly speaking, our study demonstrates that the Pliocene provides meaningful insights into near-future climate change.

Acknowledgments

We thank Harry Dowsett, Dan Lunt, and an anonymous reviewer for comments and suggestions that improved the manuscript. We thank Kira Lawrence and Antoni Rosell-Melé for assistance in compiling the alkenone data. We thank Kevin Anchukaitis for comments and input. Funding for this research was provided by the David and Lucile Packard Foundation Fellowship in Science and Engineering to J. E. T. Authors B. O.-B. and R. F. acknowledge support by the National Center for Atmospheric Research, which is a major facility sponsored by the U.S. National Science Foundation under Cooperative Agreement 1852977 and additionally by NSF-EAR Award 1237211. The CESM project is supported primarily by the National Science Foundation. Computing resources (<https://doi.org/10.5065/D6RX99HX>) were provided by the Climate Simulation Laboratory at NCAR's Computational and Information Systems Laboratory, sponsored by the National Science Foundation and other agencies. The compiled proxy data, regional reconstructions of SST anomalies, and reduced space field reconstruction are available as Data Sets S1–S3 attached to this manuscript and are also archived in the PANGAEA database (<https://pangaea.de>). CESM-CAM5 RCP2.6 model results are available on the Earth System Grid (<https://www.earthsystemgrid.org/>). PlioMIP model output is available upon request to A. M. H. (A.M.Haywood@leeds.ac.uk). CESM-CAM5 Pliocene model results are available upon request to R. F. (ran.feng@uconn.edu). BAYSPLINE code is publicly available for download online (<https://github.com/jesstierney/BAYSPLINE>).

References

- Bretherton, C. S. (2015). Insights into low-latitude cloud feedbacks from high-resolution models. *Philosophical Transactions of the Royal Society A*, 373, 20140415.
- Brierley, C. (2015). Interannual climate variability seen in the Pliocene Model Intercomparison Project. *Climate of the Past*, 11(3), 605–618.
- Brierley, C., Burls, N., Ravelo, C., & Fedorov, A. (2015). Pliocene warmth and gradients. *Nature Geoscience*, 8(6), 419–420.
- Burls, N., & Fedorov, A. (2014). Simulating Pliocene warmth and a permanent El Niño-like state: The role of cloud albedo. *Paleoceanography*, 29, 893–910. <https://doi.org/10.1002/2014PA002644>
- Burls, N. J., & Fedorov, A. V. (2017). Wetter subtropics in a warmer world: Contrasting past and future hydrological cycles. *Proceedings of the National Academy of Sciences*, 114(49), 12,888–12,893.
- Chung, E.-S., Timmermann, A., Soden, B. J., Ha, K.-J., Shi, L., & John, V. O. (2019). Reconciling opposing Walker circulation trends in observations and model projections. *Nature Climate Change*, 9(5), 405–412.
- Clement, A. C., Burgman, R., & Norris, J. R. (2009). Observational and model evidence for positive low-level cloud feedback. *Science*, 325(5939), 460–464.
- DiNezio, P. N., Clement, A. C., Vecchi, G. A., Soden, B. J., Kirtman, B. P., & Lee, S.-K. (2009). Climate response of the equatorial Pacific to global warming. *Journal of Climate*, 22(18), 4873–4892.
- Dowsett, H. (2007). Faunal re-evaluation of Mid-Pliocene conditions in the western equatorial Pacific. *Micropaleontology*, 53(6), 447–456.
- Dowsett, H. J., Haywood, A. M., Valdes, P. J., Robinson, M. M., Lunt, D. J., Hill, D. J., et al. (2011). Sea surface temperatures of the mid-Piacenzian Warm Period: A comparison of PRISM3 and HadCM3. *Palaeogeography, Palaeoclimatology, Palaeoecology*, 309(1–2), 83–91.
- Dowsett, H., Robinson, M., & Foley, K. (2009). Pliocene three-dimensional global ocean temperature reconstruction. *Climate of the Past*, 5(4), 769–783.
- Dowsett, H., Robinson, M., Haywood, A., Salzmann, U., Hill, D., Sohl, L., et al. (2010). The PRISM3D paleoenvironmental reconstruction. *Stratigraphy*, 7(2–3), 123–139.
- Emanuel, K., Sundararajan, R., & Williams, J. (2008). Hurricanes and global warming: Results from downscaling IPCC AR4 simulations. *Bulletin of the American Meteorological Society*, 89(3), 347–367.
- Evans, D., Brierley, C., Raymo, M. E., Erez, J., & Müller, W. (2016). Planktic foraminifera shell chemistry response to seawater chemistry: Pliocene–Pleistocene seawater Mg/Ca, temperature and sea level change. *Earth and Planetary Science Letters*, 438, 139–148.
- Fedorov, A. V., Brierley, C. M., & Emanuel, K. (2010). Tropical cyclones and permanent El Niño in the early Pliocene epoch. *Nature*, 463(7284), 1066.
- Fedorov, A. V., Burls, N. J., Lawrence, K. T., & Peterson, L. C. (2015). Tightly linked zonal and meridional sea surface temperature gradients over the past five million years. *Nature Geoscience*, 8(12), 975.
- Fedorov, A., Dekens, P., McCarthy, M., Ravelo, A., Barreiro, M., Pacanowski, R., & Philander, S. (2006). The Pliocene paradox (mechanisms for a permanent El Niño). *Science*, 312(5779), 1485–1489.
- Foster, G. L., Royer, D. L., & Lunt, D. J. (2017). Future climate forcing potentially without precedent in the last 420 million years. *Nature Communications*, 8, 14845.
- Gettelman, A. (2015). Putting the clouds back in aerosol–cloud interactions. *Atmospheric Chemistry and Physics*, 15(21), 12,397–12,411.
- Gettelman, A., Kay, J., & Shell, K. (2012). The evolution of climate sensitivity and climate feedbacks in the Community Atmosphere Model. *Journal of Climate*, 25(5), 1453–1469.
- Gill, E. C., Rajagopalan, B., Molnar, P., & Marchitto, T. M. (2016). Reduced-dimension reconstruction of the equatorial Pacific SST and zonal wind fields over the past 10,000 years using Mg/Ca and alkenone records. *Paleoceanography*, 31, 928–952. <https://doi.org/10.1002/2016pa002948>
- Gray, W. R., Weldeab, S., Lea, D. W., Rosenthal, Y., Gruber, N., Donner, B., & Fischer, G. (2018). The effects of temperature, salinity, and the carbonate system on Mg/Ca in Globigerinoides ruber (white): A global sediment trap calibration. *Earth and Planetary Science Letters*, 482, 607–620.
- Haywood, A., Dowsett, H., Otto-Bliesner, B., Chandler, M., Dolan, A., Hill, D., et al. (2010). Pliocene Model Intercomparison Project (PlioMIP): Experimental design and boundary conditions (Experiment 1). *Geoscientific Model Development*, 3(1), 227–242.
- Haywood, A., Dowsett, H., Robinson, M., Stoll, D., Dolan, A., Lunt, D., et al. (2011). Pliocene Model Intercomparison Project (PlioMIP): Experimental design and boundary conditions (Experiment 2). *Geoscientific Model Development*, 4(3), 571–577.
- Haywood, A., Hill, D., Dolan, A., Otto-Bliesner, B., Bragg, F., Chan, W.-L., et al. (2013). Large-scale features of Pliocene climate: Results from the Pliocene Model Intercomparison Project. *Climate of the Past*, 9(1), 191.
- Huang, B., Thorne, P. W., Banzon, V. F., Boyer, T., Chepurin, G., Lawrimore, J. H., et al. (2017). Extended reconstructed sea surface temperature, version 5 (ERSSTv5): Upgrades, validations, and intercomparisons. *Journal of Climate*, 30(20), 8179–8205.
- Hurrell, J. W., Holland, M. M., Gent, P. R., Ghan, S., Kay, J. E., Kushner, P. J., et al. (2013). The Community Earth System Model: A framework for collaborative research. *Bulletin of the American Meteorological Society*, 94(9), 1339–1360.
- Karnauskas, K. B., Seager, R., Kaplan, A., Kushnir, Y., & Cane, M. A. (2009). Observed strengthening of the zonal sea surface temperature gradient across the equatorial Pacific Ocean. *Journal of Climate*, 22(16), 4316–4321.
- Knutson, T. R., & Manabe, S. (1995). Time-mean response over the tropical Pacific to increased CO₂ in a coupled ocean-atmosphere model. *Journal of Climate*, 8(9), 2181–2199.
- L'Heureux, M. L., Lee, S., & Lyon, B. (2013). Recent multidecadal strengthening of the Walker circulation across the tropical Pacific. *Nature Climate Change*, 3(6), 571.

- Lau, N.-C., & Nath, M. J. (1996). The role of the “atmospheric bridge” in linking tropical Pacific ENSO events to extratropical SST anomalies. *Journal of Climate*, *9*(9), 2036–2057.
- Li, G., Xie, S.-P., Du, Y., & Luo, Y. (2016). Effects of excessive equatorial cold tongue bias on the projections of tropical Pacific climate change. Part I: The warming pattern in CMIP5 multi-model ensemble. *Climate Dynamics*, *47*(12), 3817–3831.
- Lunt, D. J., Haywood, A. M., Schmidt, G. A., Salzmann, U., Valdes, P. J., Dowsett, H. J., & Loptson, C. A. (2012). On the causes of mid-Pliocene warmth and polar amplification. *Earth and Planetary Science Letters*, *321*, 128–138.
- Meinshausen, M., Smith, S. J., Calvin, K., Daniel, J. S., Kainuma, M., Lamarque, J.-F., et al. (2011). The RCP greenhouse gas concentrations and their extensions from 1765 to 2300. *Climatic Change*, *109*(1-2), 213.
- Müller, P., Kirst, G., Ruhland, G., Von Storch, I., & Rosell-Melé, A. (1998). Calibration of the alkenone paleotemperature index $U_{37}^{K'}$ based on core-tops from the eastern South Atlantic and the global ocean (60°N–60°S). *Geochimica et Cosmochimica Acta*, *62*(10), 1757–1772.
- O'Brien, C. L., Foster, G. L., Martínez-Botí, M. A., Abell, R., Rae, J. W., & Pancost, R. D. (2014). High sea surface temperatures in tropical warm pools during the Pliocene. *Nature Geoscience*, *7*(8), 606–611.
- Ravelo, A. C., Lawrence, K. T., Fedorov, A., & Ford, H. L. (2014). Comment on “A 12-million-year temperature history of the tropical Pacific Ocean”. *Science*, *346*(6216), 1467–1467.
- Regenberg, M., Regenberg, A., Garbe-Schönberg, D., & Lea, D. W. (2014). Global dissolution effects on planktonic foraminiferal Mg/Ca ratios controlled by the calcite-saturation state of bottom waters. *Paleoceanography*, *29*, 127–142. <https://doi.org/10.1002/2013pa002492>
- Schneider, T., Kaul, C. M., & Pressel, K. G. (2019). Possible climate transitions from breakup of stratocumulus decks under greenhouse warming. *Nature Geoscience*, *12*(3), 163.
- Seager, R., Cane, M., Henderson, N., Lee, D.-E., Abernathy, R., & Zhang, H. (2019). Strengthening tropical Pacific zonal sea surface temperature gradient consistent with rising greenhouse gases. *Nature Climate Change*, *9*(7), 517–522.
- Taylor, K. E., Stouffer, R. J., & Meehl, G. A. (2012). An overview of CMIP5 and the experiment design. *Bulletin of the American Meteorological Society*, *93*(4), 485–498.
- Tierney, J. E., & Tingley, M. P. (2018). BAYSPLINE: A new calibration for the alkenone paleothermometer. *Paleoceanography and Paleoclimatology*, *33*(3), 281–301.
- Vecchi, G. A., & Soden, B. J. (2007). Global warming and the weakening of the tropical circulation. *Journal of Climate*, *20*(17), 4316–4340.
- Wara, M. W., Ravelo, A. C., & Delaney, M. L. (2005). Permanent El Niño-like conditions during the Pliocene warm period. *Science*, *309*(5735), 758–761.
- Watanabe, T., Suzuki, A., Minobe, S., Kawashima, T., Kameo, K., Minoshima, K., et al. (2011). Permanent El Niño during the Pliocene warm period not supported by coral evidence. *Nature*, *471*(7337), 209.
- Zhang, Y. G., Pagani, M., & Liu, Z. (2014). A 12-million-year temperature history of the tropical Pacific Ocean. *Science*, *344*(6179), 84–87.